5 Experimental Verification

5.1. Purpose

The purpose of the experimental verification is to verify the analytical results by experimental procedures and results. The experimental verification is performed to make sure that the concept functions according to design specifications, and to be able to explain any deviations from the theoretical predictions.

The experimental verification is also performed to characterize the design parameters, like mass, stiffness and damping constants. These parameters, especially damping and stiffness, will definitely be frequency dependent, and the results from the experimental procedure will be used to update the design parameters.

The experimental procedure will also be used as an opportunity to review the design in terms of certain practical problems that appear during the course of the tests. These problems will be stated in the evaluation, and also the corrective actions that have been taken to overcome them.

To summarise, the experimental verification will be used to learn more about the concept's abilities and limitations. Also to evaluate which predictions and assumptions made in the mathematical modeling and design were correct, and which would have to be revised. The design has been done in such a way that various parameters and elements can be changed, to ensure that the performance of this concept can be described in terms of most of the critical variables.

5.2. Measurement of inertial properties

The system is characterised by three important parameters: mass, stiffness and damping. The stiffness coefficient will be dealt with in section 5.3, and the damping coefficient is calculated in section 5.5. The mass includes the mass of the handle and port assembly, the mass of the housing and mounting plates, and the mass of the fluid inside the port

The masses of the steel components were measured on an electronic scale, and the results were as follows:
Handle and port assembly: ca. 1.7 kg
Bottom housing and cover plate: ca. 3.4 kg

Two different fluids were used during the tests, a water and anti-freeze mixture, and methylated spirits. The densities of these fluids were measured as:
Water mixture: 1043 kg/m^3
Methylated spirits: 840 kg/m^3
These measurements were done by measuring the mass of a known volume of the substance on an electronic scale.

The mass of the fluid in the port can be calculated by

$$m_2 = \rho \cdot a \cdot L \qquad (5.1)$$

Three different port diameters were used, and for the water mixture the mass of the fluid in the port was:
10 mm port: 2.45 g
12.5 mm port 3.84 g
20 mm port 9.83 g

5.3. Experimental procedure

The tests on the handle were done by exciting the structure at the attachment point by using a hydraulic actuator, and at the same time measuring the response of the handle. At this stage it is important to define the characteristics of the systems that have to be evaluated with the results of the tests. The most important characteristic of the system is the transmissibility function. The transmissibility reveals the isolation frequency, and the frequency of maximum force transfer. Other important characteristics are physical constants like stiffness and damping. These constants are important for the comparison of the analytical predictions with the theoretical results.

5.3.1 Force measurement

Consider the figure in Fig. 5.1. The figure represents the first part of the experimental procedure, where the handle is restrained, and the housing is excited. This part will be referred to as the force measurement. The measured quantities are printed in bold.

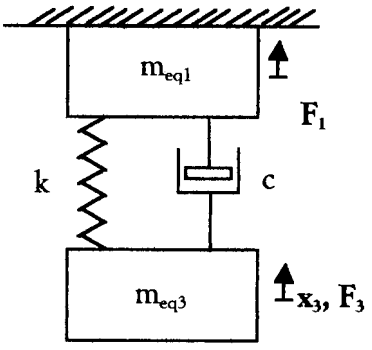

Figure 5.1: Representation of force measurement

The force measurement procedure will be used to calculate the transmissibility and stiffness coefficient of the system. A transmissibility function can be calculated if the measured response is divided by a known or measured input:

$T_r = \frac{F_1}{F_3}$, where F_1 is the force measured on the handle, and F_3 is the force exerted by the actuator.

Stiffness coefficient

The stiffness includes the stiffness of the polyurethane rubber, and that of the diaphragm above the port. The stiffness can be calculated by evaluating the real part of the equation:

$$k = -m_{eq3} \cdot \omega^2 + i \cdot \omega \cdot c - \frac{F_3}{X_3} \qquad (5.2)$$

The force F_3 is the force that the actuator exerts on the system.

Damping coefficient

The damping includes the structural damping of the polyurethane rubber, the fluid losses in the port, the structural damping of the diaphragm above the port, and the damping of the moving air above the diaphragm. The results of the damping coefficient in terms of frequency were not satisfying enough, and the reason for this will be discussed at the end of this chapter. A modal method described by Rao (1995:659) is used to determine the approximate the damping coefficient. The equation

$$\zeta = \frac{\omega_2 - \omega_1}{2\omega_n} \tag{5.4}$$

can be used to calculate the damping ratio. ω_1 and ω_2 are the frequencies corresponding to the half power points of the frequency response function X_3/F_3 (see figure 5.11). The damping coefficient can be calculated with

$$c = 2 \cdot m \cdot \omega_n \cdot \zeta \tag{5.5}$$

5.3.2 Acceleration measurements

The second part of the experimental procedure is schematically shown in Fig. 5.2, and will be referred to as the acceleration measurement.

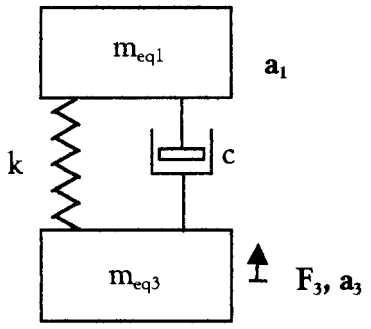

Figure 5.2: Representation of acceleration measurement

During this stage, the handle was free to move during the excitation of the base m_{eq3}. The accelerations of the handle and that of the base were measured. The force exerted on the base by the actuator was also measured. This procedure was performed to confirm the transfer function by using other equipment, and to evaluate the change in attenuation. This will hypothetically also be the operation of such a design on a rock drill, and it would thus be sensible to evaluate the response of the system in such a configuration.

The transmissibility function can be calculated as:

$$T_r = \frac{a_1}{a_3} \tag{5.3}$$

where a_3 is the input acceleration. The damping and stiffness of the system can be calculated by modal analysis methods, but it should be remembered that the these parameters are frequency dependent and it would be a linear estimation of a non-linear system. The non-linearity is primarily due to the rubber elements used in the system.

5.4. Experimental setup

A schematic representation of the force measurement experimental setup is shown in Fig. 5.3, while a photo can be seen in Fig. 5.4. The input signal to the actuator is generated in MATLAB and fed into the controller via the CDAS D/A converter card. The CDAS converter card has 6 input A/D channels and 2 D/A channels. The CDAS has all the appropriate anti-aliasing filters, and can be seen in Fig. 5.5. The controller controls the displacement of the servo valve of the actuator. The controller also controls the minimum and maximum displacement of the actuator. The motion of the actuator is measured by LVDT, and fed into the computer via the CDAS. The top and bottom load cells (F_1 and F_3) are fed via separate amplifiers into the computer for recording. The operating range of the servo valve is 0-100 Hz, and the maximum force on the load cells is 5 tons.

The input signals for this configuration were sine and sine sweep signals of approximately 60 seconds in duration. The first measurements were done by only one sweep, but as the coherence lowered at the later stages of the force measurements, an average over five sweeps was taken. Random signals were also generated, but the resulting measurements were not satisfactory. This could also be due to the phase difference of the amplifiers discussed later in this chapter (see results: Acceleration measurements, pp 83).

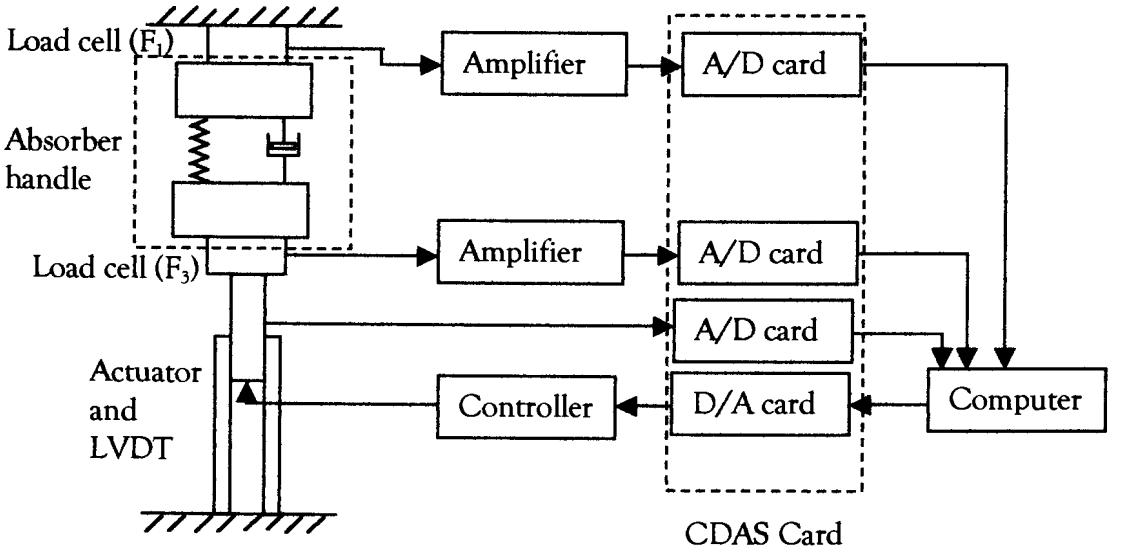

Figure 5.3: Force measurement experimental setup

The measurements were immediately in MATLAB format, and could be processed in the same program. Measurements ranged between 0 and 100 Hz with a sampling

frequency of 1000 Hz. Figures 5.4 to 5.6 show photographs of the force measurement setup.

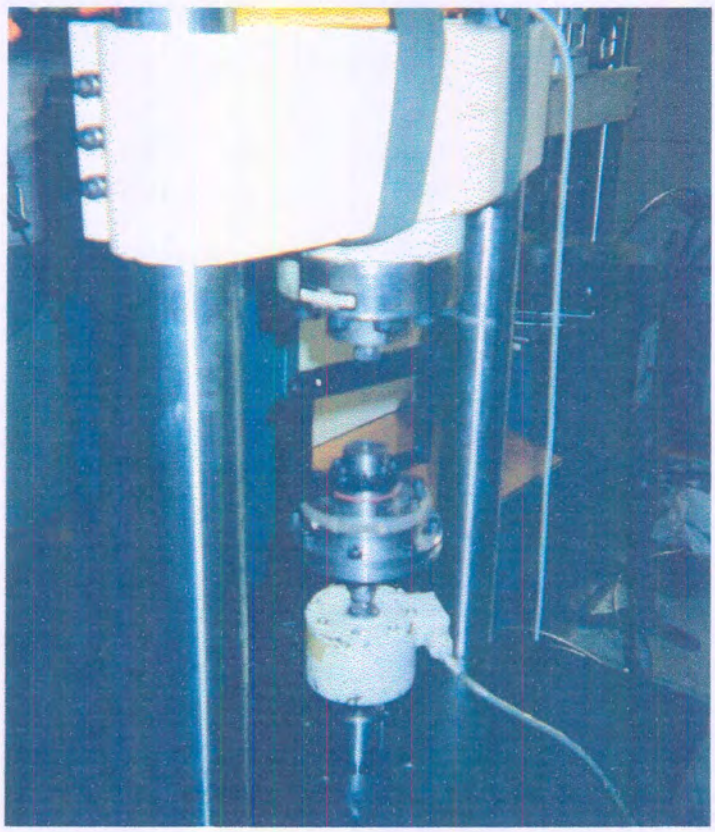

Figure 5.4: Force measurement

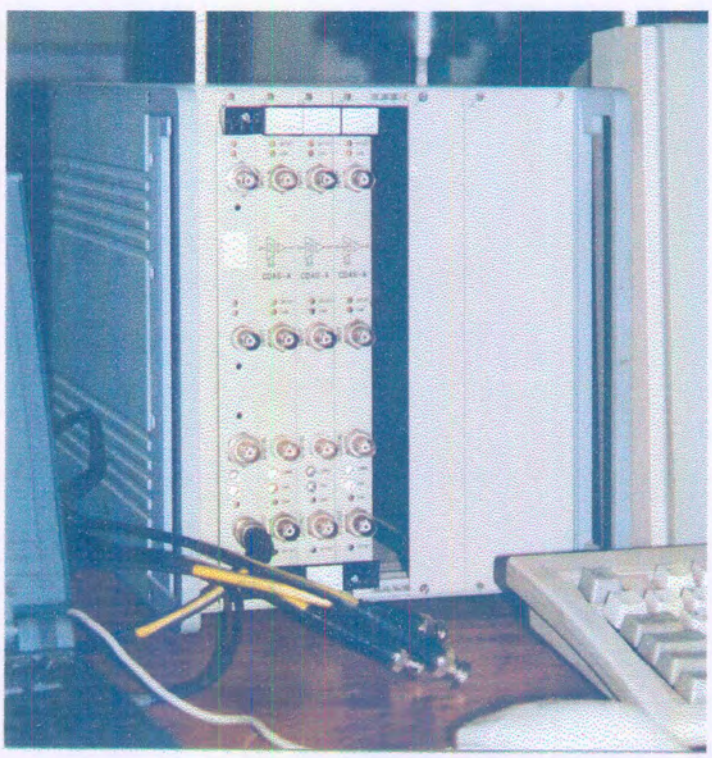

Figure 5.5: CDAS controller

The acceleration measurement setup is shown in fig 5.6 and 5.7.

As previously described, the absorber handle was not constrained in this configuration. The PCB miniature high frequency 10 mV/g accelerometers (Model 353 B17) were mounted at the top and at the bottom. These accelerometers sent an analogue signal via the amplifiers to the Siglab analyser. This analyser converted the signal to digital format and fed it into the computer for recording. The load cell operated through a separate amplifier, but the signal conditioning was also done by the Siglab analyser.

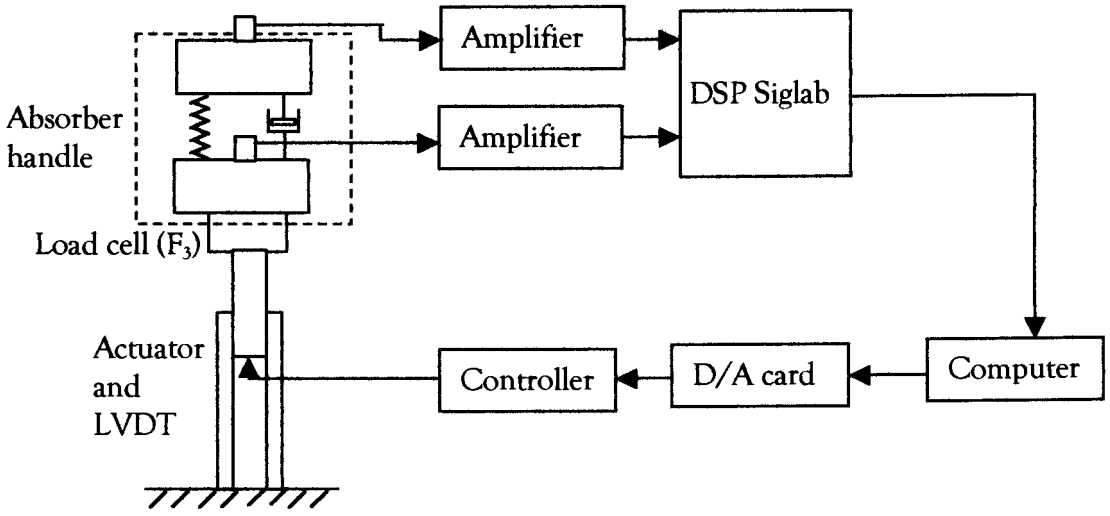

Figure 5.6: Acceleration measurement experimental setup

The input to the actuator was done through the controller via the CDAS converter card, and was band-limited random signals. These signals were generally limited between 5 and 90 Hz with a RMS amplitude varying between 0.5 and 1.5 mm amplitude. The compensation for the apparent mass of the operator's hand-arm system was done by a weight mounted onto the handle of the absorber (Fig. 5.7).

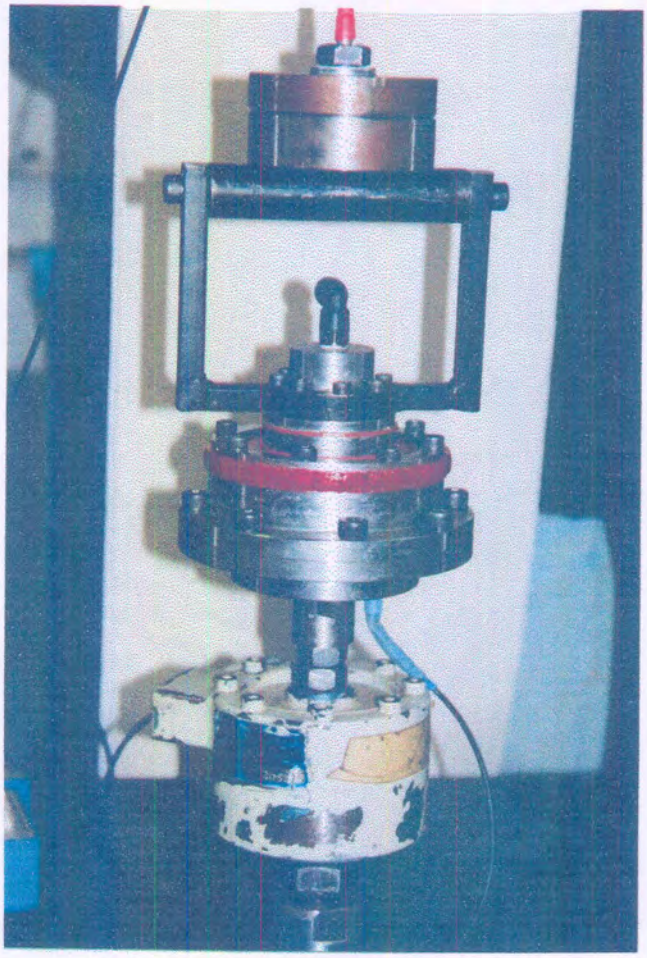

Figure 5.7: Acceleration measurement

5.5. Results

Force measurements

The force measurement was done according to the procedure described in section 5.3.1. This was mainly a characterisation phase during which the system's variables, the stiffness and damping coefficients, were evaluated. These parameters, although estimated during the design phase in chapter 4, were quite different from what had been expected. The theoretical model derived in chapter 4 will thus constantly be updated with the experimentally obtained stiffness and damping coefficients in order to accurately validate the model.

Due to the above-mentioned facts, the isolation frequency has also not been situated at the predicted frequency, and certain parameters like port diameter and diaphragm stiffness have been changed in order to move the isolation frequency to the desired value, which is between 30 and 35 Hz.

System without absorbing fluid

The first results that will be represented, is the response of the system without any fluid inside the absorber. This system can be modelled as a single-degree-of-freedom system,

and the stiffness and damping of the polyurethane rubber can be calculated with these results. An important factor that should be remembered is that the system with fluid inside is much stiffer than the system without fluid inside, due to the added stiffness of the diaphragm. This increase in stiffness due to the diaphragm could not be accurately modelled in the design phase, and the theoretical model will thus be updated after the stiffness of the diaphragm has been calculated.

Transmissibility

The data as received from the CDAS converter card is time domain signals that are filtered with a low-pass filter below 100 Hz. The transmissibility is then calculated by using MATLAB. The transmissibility plot for the system without absorbing fluid is shown is given in Fig. 5.9.

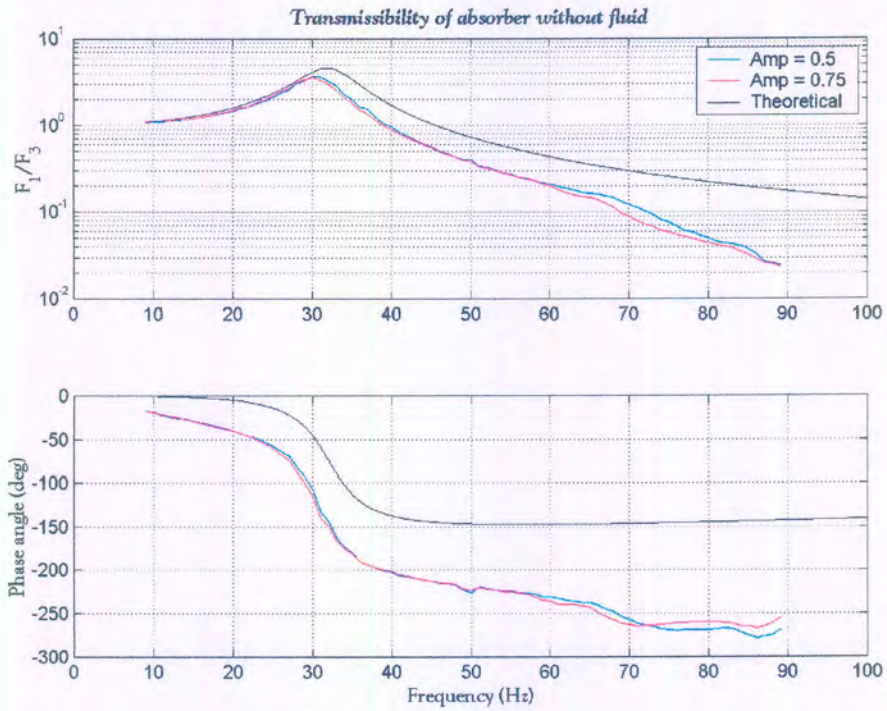

Figure 5.9: System without fluid - Transmissibility

Two amplitudes were used as excitation, nominally 0.5 and 0.75 mm sine sweeps, although the actuator cannot maintain the specified amplitude constant during the entire sweep. The frequency of the sine sweeps was linearly increasing from 0 to 90 Hz.

The system shows, as expected, the characteristics of a single-degree-of-freedom system, with a MT frequency at about 30 Hz. The variation with amplitude of excitation is negligible. The theoretical estimation is also shown in Fig. 5.9. The stiffness coefficient was taken as 100 kN/m, acquired from the graph in Fig. 5.10 at the MT frequency of the system. The damping coefficient was taken as 107 Ns/m as calculated below. The mass used for the theoretical estimation was taken as 2.43, which represents the bottom part of the absorber as calculated in section 4.6.

Stiffness coefficient

The stiffness coefficient was calculated by using eq. 5.2. Fig. 5.10 shows a plot of the stiffness coefficient vs. frequency for the two excitation amplitudes.

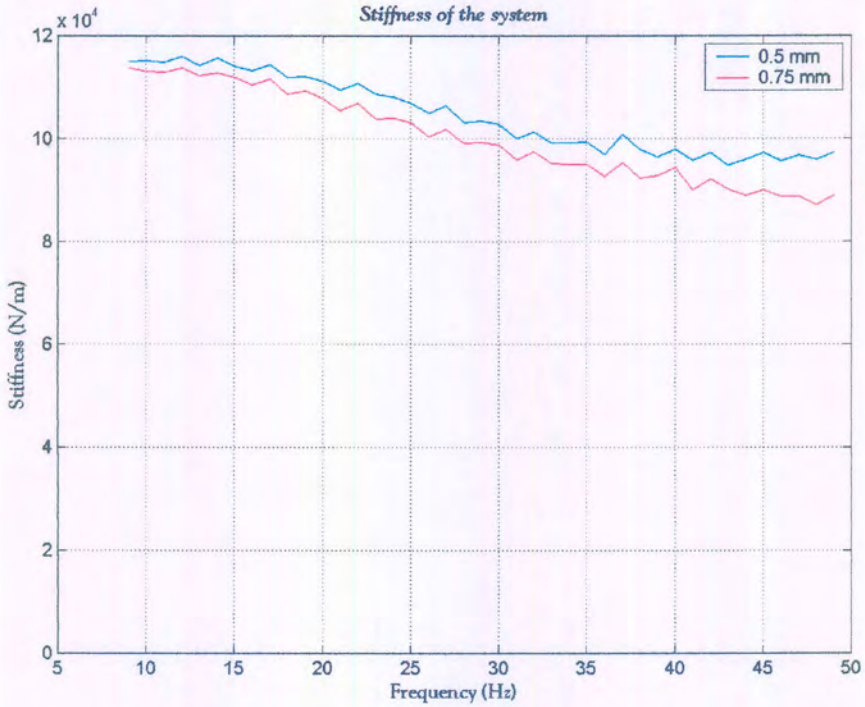

Figure 5.10: System without fluid – Stiffness constant

The figure represents the stiffness of the polyurethane rubber, and shows that the stiffness constant changes with about 30 kN/m over a frequency range of 40 Hz. The static stiffness is between 115 and 120 kN/m.

Damping coefficient

Although the damping coefficient would be frequency dependent, the value near the MT frequency is certainly the most important. Using eqs. 5.4 and 5.5, the damping coefficients for two amplitudes, 0.5 and 0.75 mm, are 128.965 and 107.38 Ns/m respectively. The hysteresis damping coefficient can be evaluated as (Rao, 1995: 224)

$$\beta = \frac{c\omega}{k} \qquad (5.6)$$

The value of this coefficient at the MT frequency for the two amplitudes, 0,5 and 0,75 mm, are 0,2213 and 0,1906 respectively. It is important to remember that eq. 5.4 is only an approximation.

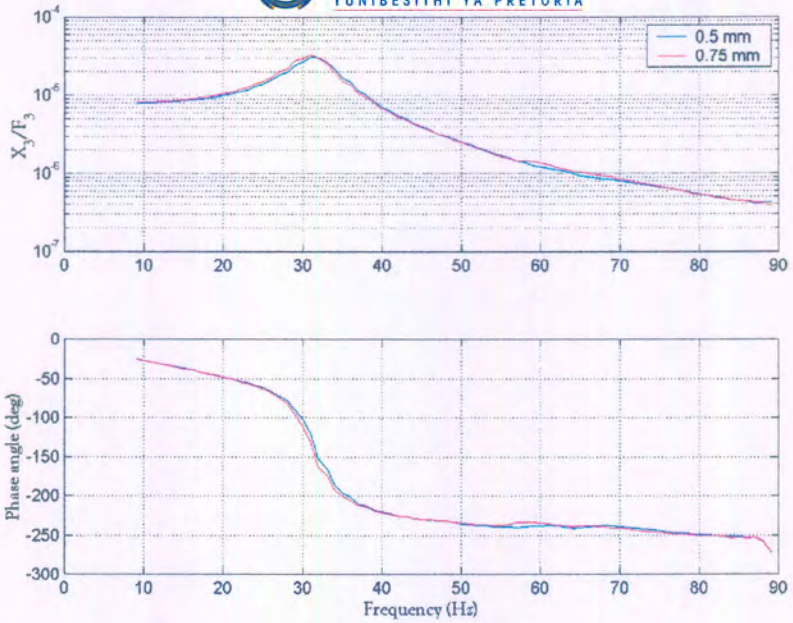

Figure 5.11: System without fluid - Transfer function

An interesting point to notice when looking at Fig. 5.11 is the fact that the resonant frequency is the same as the MT frequency. This is probably due to the simplicity of the system.

Coherence

Coherence is very important to ensure that the data and further processing thereof are reliable and representative. The coherence data for the transmissibility is plotted in Fig. 5.12. The coherence of the transmissibility is good at most frequencies, only falling at the natural frequency, which is normal, and at the Eskom supply frequency of 50 Hz.

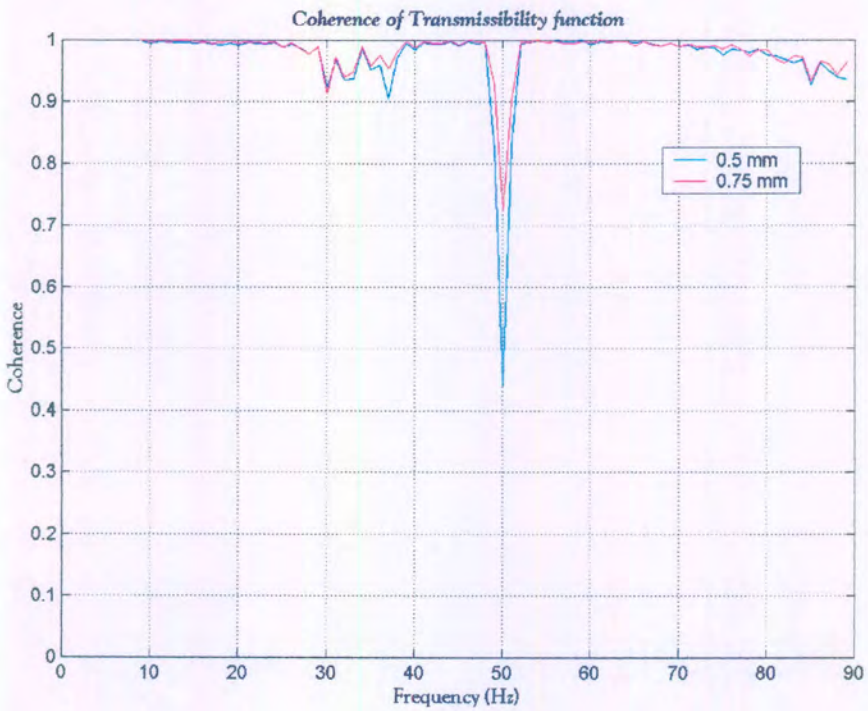

Figure 5.12: System without fluid - Coherence

The coherence also falls a bit at higher frequencies, which is probably due to the fact that the servo valve is not so dependable at frequencies above 80 Hz.

System with water mixture as absorbing fluid and 0.02 mm port

The first absorbing configuration that was tested used the water mixture as the absorbing fluid. The large 0.02 mm port was used, and a stiff 0.002 mm thick rubber as a diaphragm. The results obtained from this test were not very good compared to the rest of the measurements, due to the fact that the isolation frequency is situated at about 80 Hz. As seen in the previous section, the coherence is already lower at higher frequencies, and the isolation frequency lowers the coherence even further. The important aspects to notice at this stage, however, are that there definitely is an isolation frequency, and that the stiffness increased dramatically from the previous tests.

Transmissibility

The transmissibility plot is shown in figure 5.13. It can be seen from the figure that the isolation frequency is situated at about 80 Hz, and the MT frequency at about 47 Hz. The figure also suggests that the stiffness is a little higher with larger amplitudes and much higher than the previous configuration where there was no fluid inside the absorber. The theoretical estimation is also depicted in Fig. 5.13, and will be discussed in section 5.7.

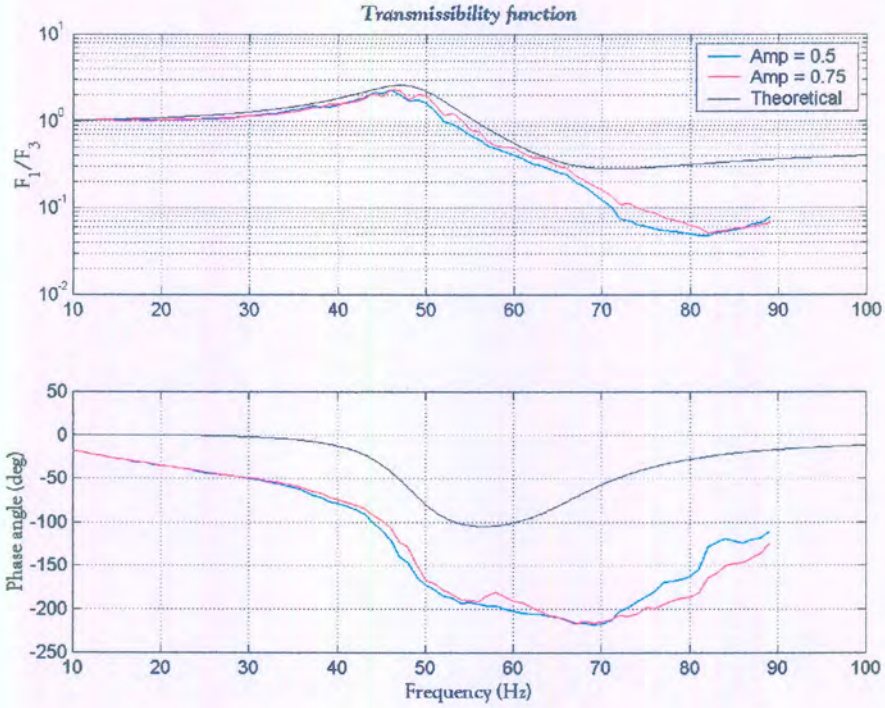

Figure 5.13: Large port with water: Transmissibility

Stiffness constant

The stiffness constant is calculated as described in the previous section. The stiffness constant for the two amplitudes is shown in Fig. 5.14. The stiffness of this configuration is about 300 kN/m static, and increases to about 550 kN/m at 50 Hz.

This is much higher than the system without an absorbing fluid, due to the effect of the diaphragm elongation; the absorber is now functioning. The stiffness also rises with frequency, unlike what was seen with the previous configuration. There is a slight difference in stiffness with different amplitudes.

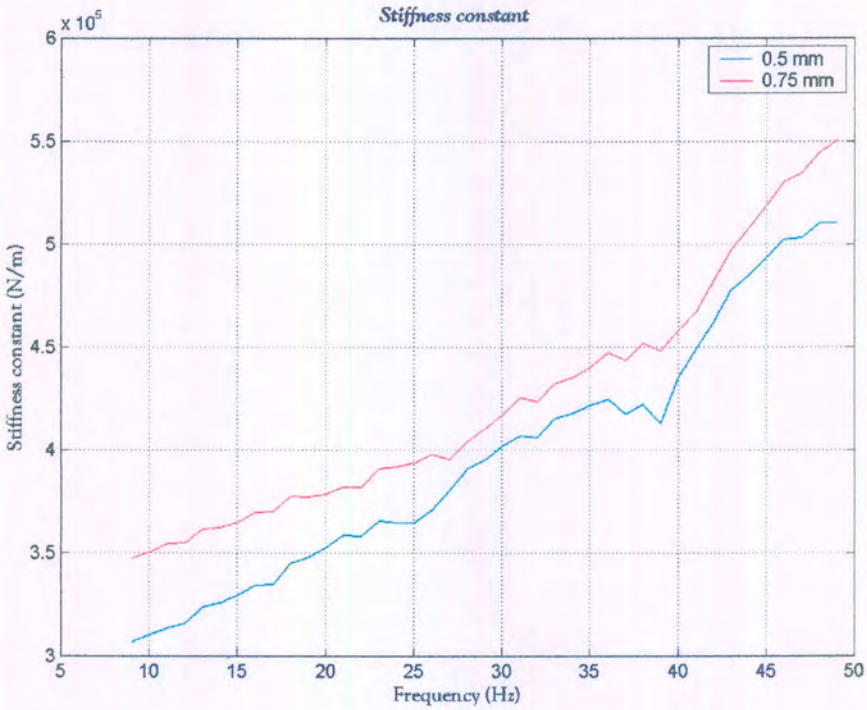

Figure 5.14: Stiffness Coefficient

Damping

The same procedure is used to calculate the damping as in the previous section. The values for the two amplitudes, 0.5 and 0.75 mm, are 366.1714 Ns/m and 457.7142 Ns/m. The variance of c in amplitude is due to the fact that the flow velocities are higher with larger amplitudes, which increase the value of the damping coefficient.

Coherence

The coherence plot for the transmissibility function is shown in Fig. 5.15. The coherence for this data set does not look very satisfactory, probably because the actuator input excitation is lower at high frequencies, and because of the fact that the isolation frequency are situated in the upper region of the frequency band. Both these phenomena causes lower signal to noise ratios.

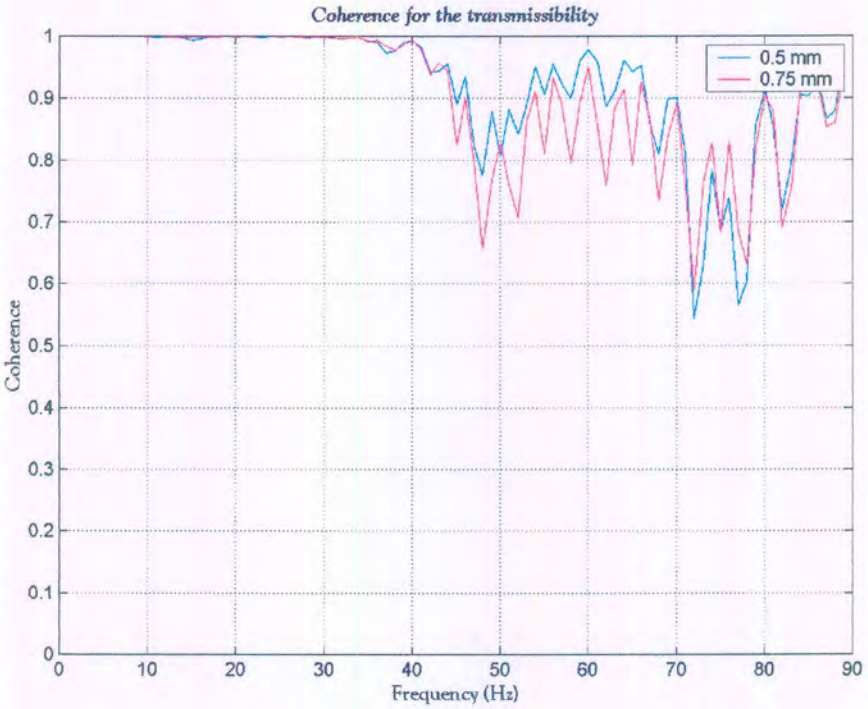

Figure 5.15: Large port with Water - Coherence

Lowering of the isolation frequency by varying certain parameters

As stated in the beginning, the isolation frequency can be lowered by changing certain parameters. The first parameter that has been changed, is the port size. The diameter of the port has been changed from 20 mm to 10 mm. This increases the area ratio of the system from 20.25 to 81. At this stage it was obvious from theoretical predictions that a 10 mm port would imply too much damping (see Fig. 5.16), and that a more flexible diaphragm with a port size between 10 and 20 mm would be the answer. This diameter value will be predicted with the mathematical model. A verification of the 10 mm port has however been considered to be important in terms of the characterisation of the design

A comparison between the transmissibility functions of the new system and the previous configuration is shown in Fig. 5.16. The isolation frequency has shifted with more than 20 Hz, but the damping has increased, and the frequency ratio (isolation frequency/MT frequency) has decreased. This has caused the amount of attenuation to decrease dramatically.

Another interesting aspect about the port change, is the change in stiffness (Fig. 5.17). The smaller port configuration is much stiffer than the large port configuration. One logical explanation for this phenomenon is that the stiff diaphragm cannot be moved away from the port. This causes the effective pressure area against the diaphragm to reduce to just about the port area. This would be especially relevant when the actuator is moving away from the handle, and the diaphragm is forced down the port throat.

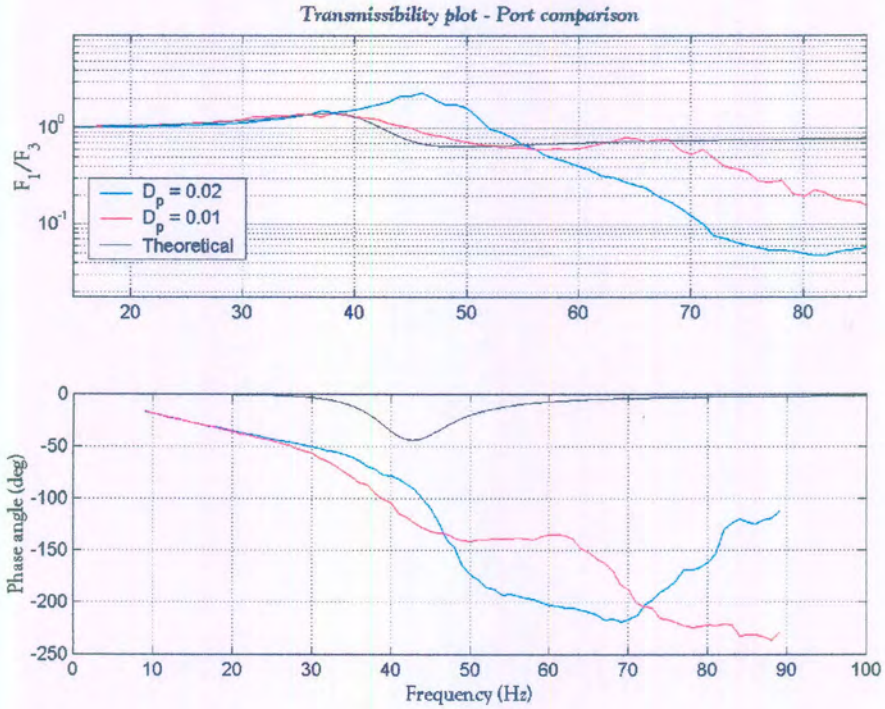

Figure 5.16: Transmissibility comparison – port variation

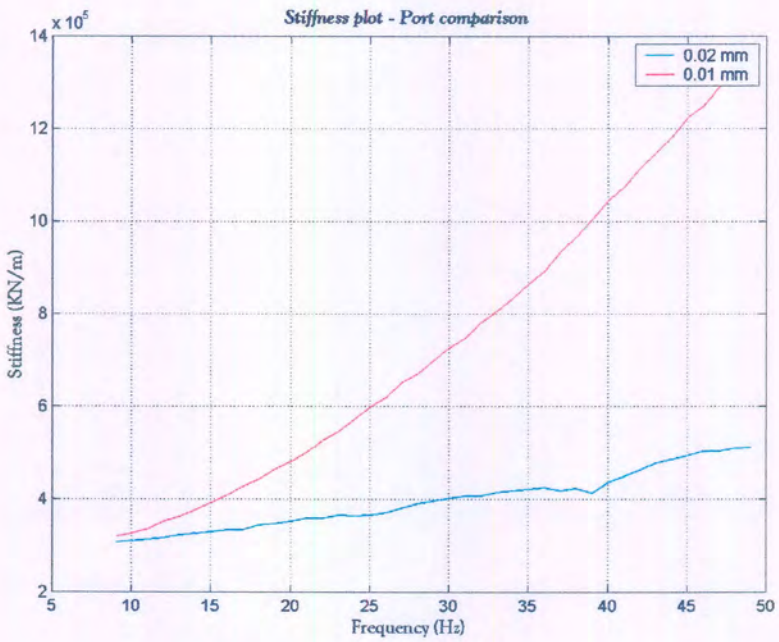

Figure 5.17: Stiffness comparison – Port variation

The next parameter that has been changed, is the diaphragm stiffness. A thinner, more flexible diaphragm has been used. The transmissibility of the new diaphragm is compared to that of the stiff diaphragm in Fig. 5.18. The port diameters are both 0.02-mm.

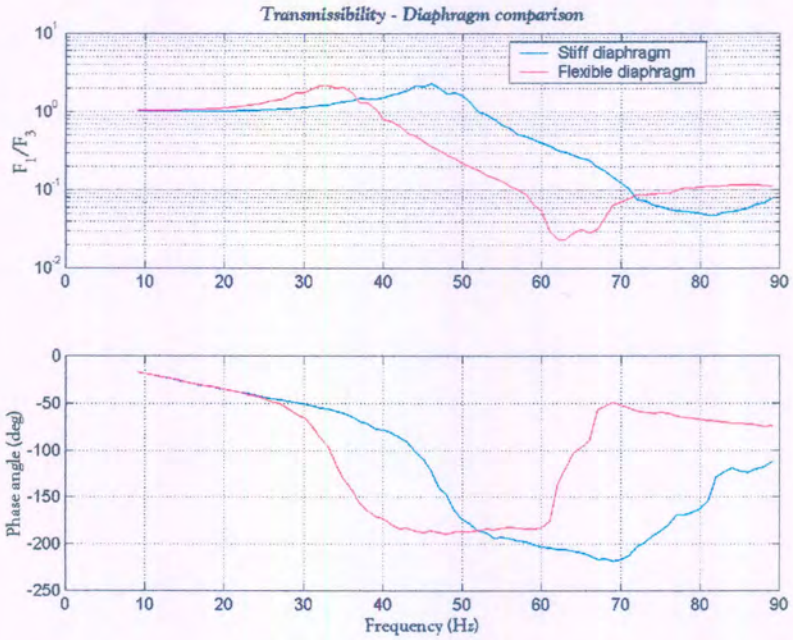

Figure 5.18: Transmissibility comparison – Diaphragm rubber variation

The isolation frequency shifted about 20 Hz with a change in diaphragm rubber. As Fig. 5.18 suggests, and Fig. 5.19 shows, the stiffness has decreased considerably.

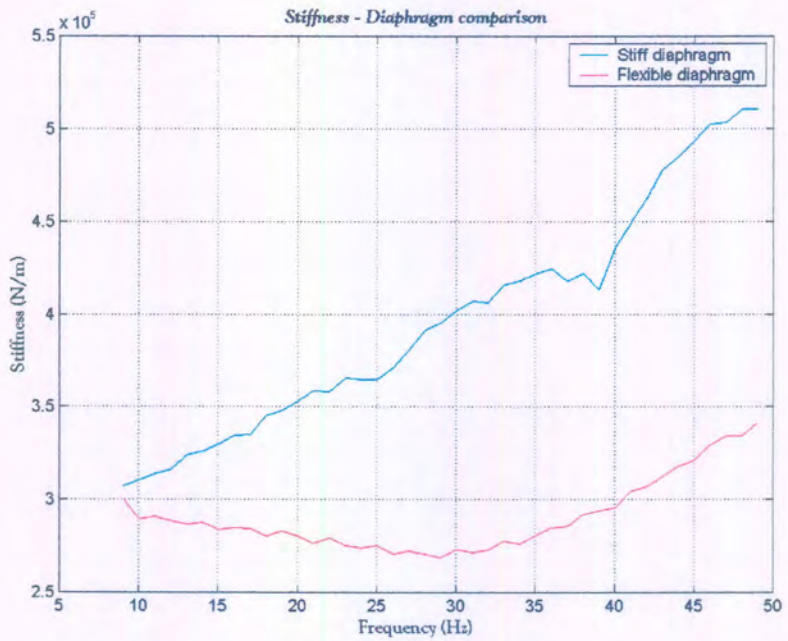

Figure 5.19: Stiffness comparison – Diaphragm variation

The next tests were done with yet a more flexible diaphragm. This diaphragm was a Latex type rubber, and was very flexible. The first test was done with the large 0.02 mm diameter port. An interesting result was obtained when the conventional diaphragm housing was removed to enlarge the pressure area on the diaphragm.

In order to shift the isolation frequency to 30 Hz with a latex rubber diaphragm, the mathematical model was used to calculate the corresponding port diameter. Fig. 5.20 shows the theoretical estimation compared to the measured data for a 12.5 mm port. The theoretical isolation frequency was calculated to be 26 Hz, in order to compensate for the fact that the stiffness will increase with a diameter reduction (Fig. 5.17).

The stiffness of the system was taken from Fig. 5.19 as 270 kN/m. The measured transmissibility is lower than the calculated transmissibility at the isolation frequency due to the fact that the ratio of ω_{MT}/ω_I is lower for the measured transmissibility because of non-linear stiffness effects.

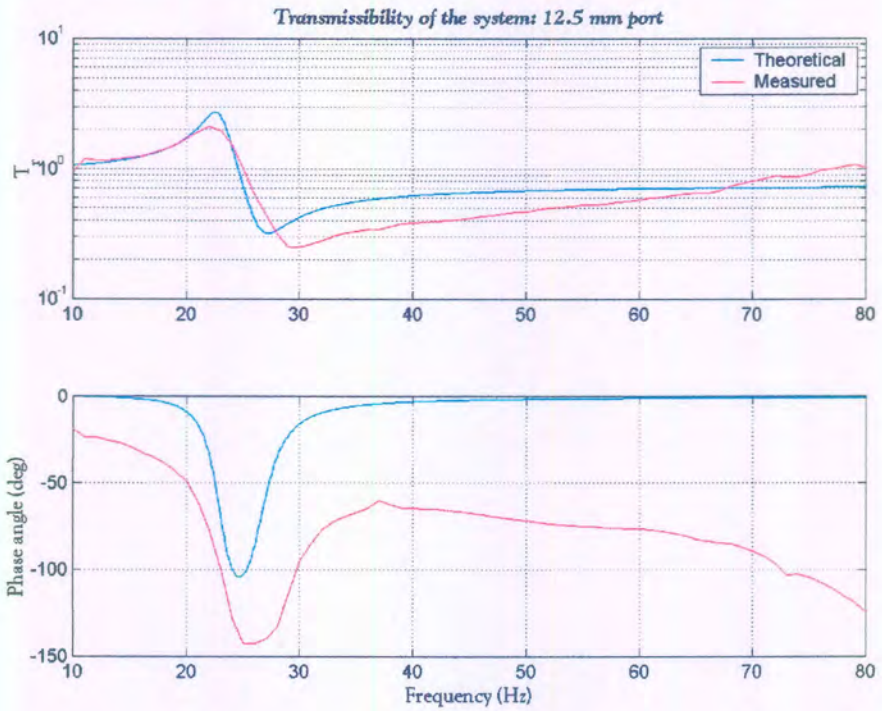

Figure 5.20: Port size verification

The transmissibility functions of three test comparisons are shown in Fig. 5.21. As the figure shows, the isolation frequency reduces when the housing is removed. The enlarged diaphragm pressure area results in a reduction in stiffness. The green line, which shows the transmissibility of the smaller port configuration, has an isolation frequency of 29 Hz. Although the transmissibility of this configuration is higher than the other two configurations, it is still only about 25 %.

The stiffness comparison is shown in Fig. 5.22. The plot shows that the stiffness of the configuration without the diaphragm is indeed lower. The stiffness of the 0.0125 mm port configuration is higher, due to the phenomenon described earlier in this chapter.

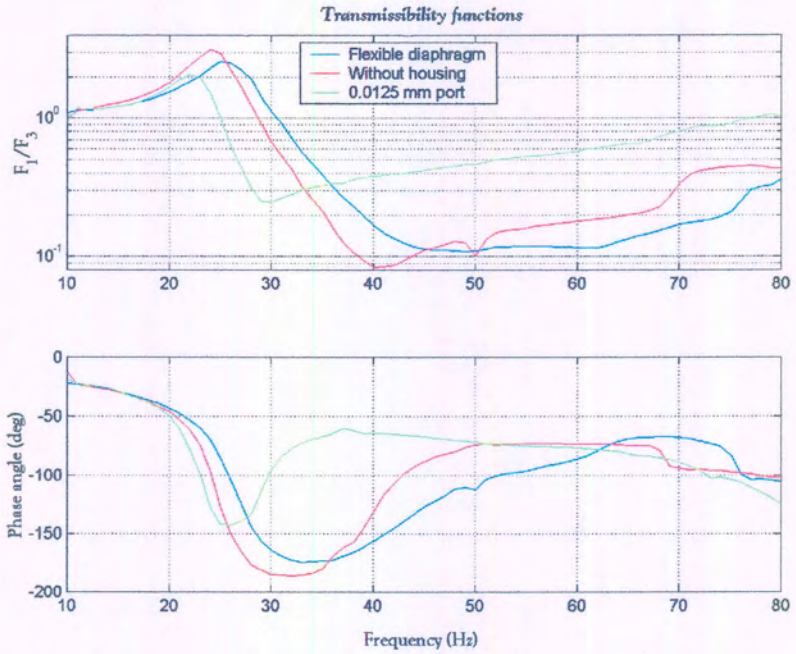

figure 5.21: Transmissibility functions of three different configurations

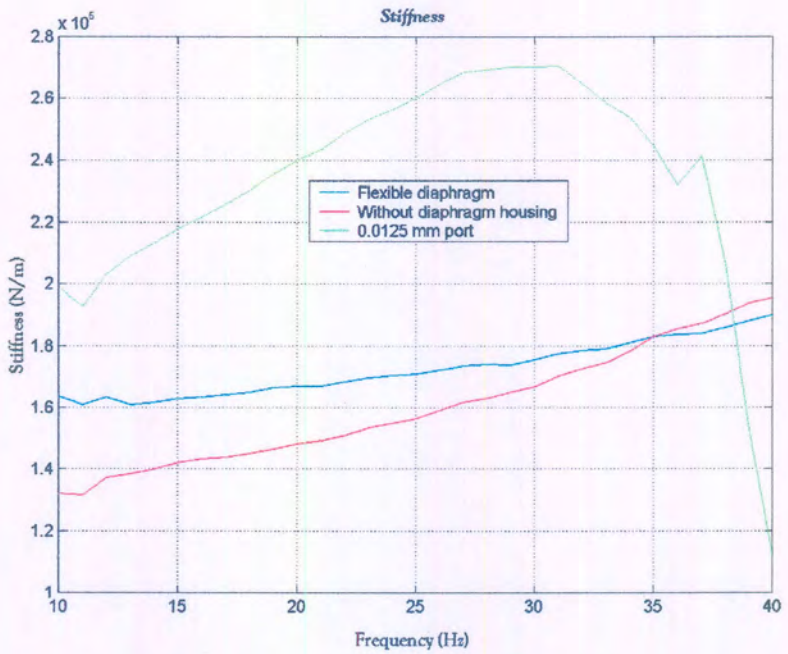

Figure 5.22: Stiffness of three different configurations

Acceleration measurements

The acceleration measurements produced much better results. As stated before, the duration of the input signal of the force measurements was 60 seconds, which was repeated five times. The five results were then averaged to produce one result that is in the time domain. The results were processed in MATLAB to produce frequency domain data. In the case of the acceleration measurements, the Siglab analyser was used. The input signal was a much longer band-limited random function, and the results were frequency domain data, already averaged 20 times. As a result, much better data was obtained.

The first configuration that was subjected to the acceleration measurements was a configuration that included a latex type diaphragm, a large port (0.02 mm diameter) and water as the absorbing fluid. The transmissibility functions for four different amplitudes (Peak – Peak values used as legend) are shown in Fig. 5.23.

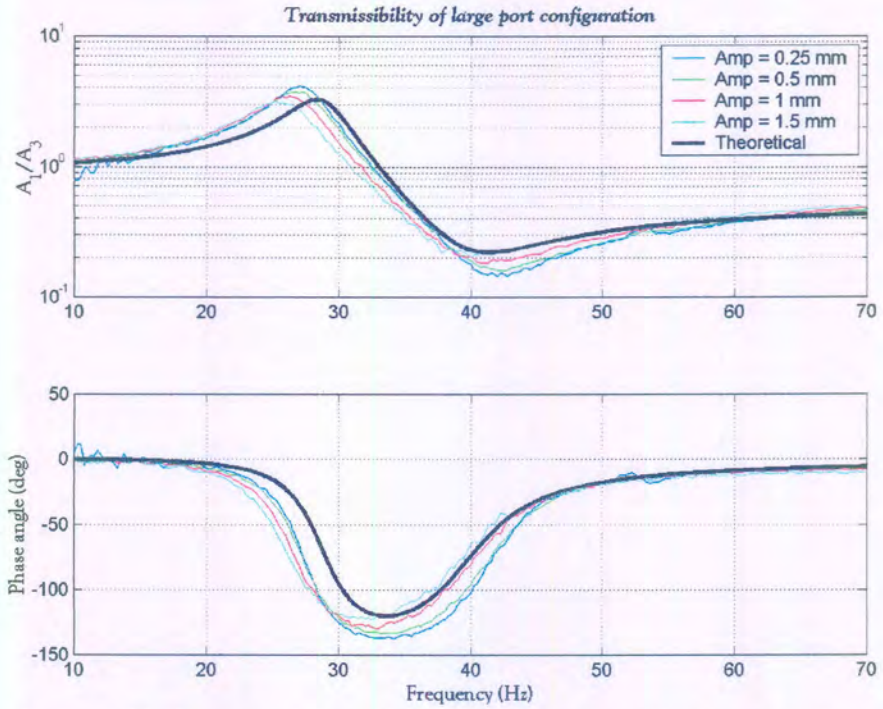

Figure 5.23: Transmissibility of large port & latex type diaphragm configuration

The isolation frequency, is just over 40 Hz, and the MT frequency is about 28 Hz. Important to notice from Fig. 5.23 is that the amplitude variation is relatively small, possibly due to small variations in stiffness and damping. The transmissibility increased slightly, due to the fact that the handle was free to translate.

The quality improvement of this measurement relative to the force measurements is clearly visible, especially when the phase angle functions are compared. The non-linear diagonal movement that was visible when the force measurements were taken, is largely eliminated. This phenomenon in the force measurements was probably due to a small phase difference between the load cell and LVDT amplifiers.

The configuration was kept the same, but the port size was changed to a 0.0125 mm diameter. The transmissibility functions of four different amplitudes (Peak – Peak values used as legend) are shown in Fig. 5.24.

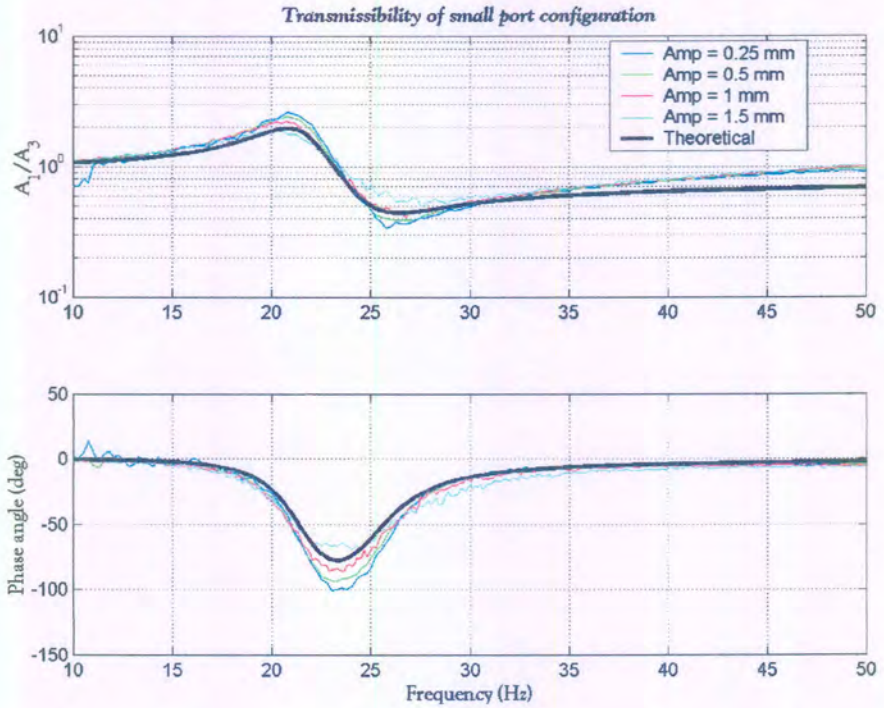

Figure 5.24: Transmissibility of small port & latex type diaphragm configuration

The isolation frequency for this configuration is about 26 Hz, and the MT frequency about 21 Hz. The minimum transmissibility for this configuration is about 40-50%.

5.6 Control system design and experimental results

The experimental results clearly show that an isolation frequency has been obtained, and also that the system responds to changes in fluid density, port diameter and stiffness. As stated in the problem specification, the system must be able to compensate for variations in the operating frequency of the rock drill due to variations in operational conditions such as pneumatic air pressure or rock hardness.

Another issue that will be addressed in this section is the problem stated in chapter 3 (Modeling of vibration absorbers) which is the problem of the MT frequency that is situated in front of the isolation frequency on the frequency spectrum. This will result in unstable or uncomfortable operating conditions during startup and hole collaring. The control system must be able to compensate for this phenomenon in a practical, suitable way.

To be able to vary the isolation frequency of the absorber, a parameter that has a noticeable effect on the isolation frequency has to be changed. The most obvious, and probably most sensitive parameter (Refer to section 4.4) is the port diameter. The port

diameter as a control variable has two important setbacks. When the port diameter is changed, the frequency ratio, γ, will change. This will cause variations in the transmissibility. The second problem is that it will be quite difficult to vary the port diameter effectively without sacrificing any sealing efficiency.

Another parameter that can cause a change in the isolation frequency is the port length. The isolation frequency will change linearly with respect to a change in port length. Although the system is not so sensitive to changes in the port length, varying the port length would probably be the easiest geometrical variable to control.

Another variable that influences both the isolation and the MT frequency, is the stiffness coefficient. The sensitivity of the isolation frequency to changes in the stiffness coefficient is not as evident as diameter variation, but on the design it would perhaps be the simplest to implement.

Compensating for unsuitable MT frequency placement

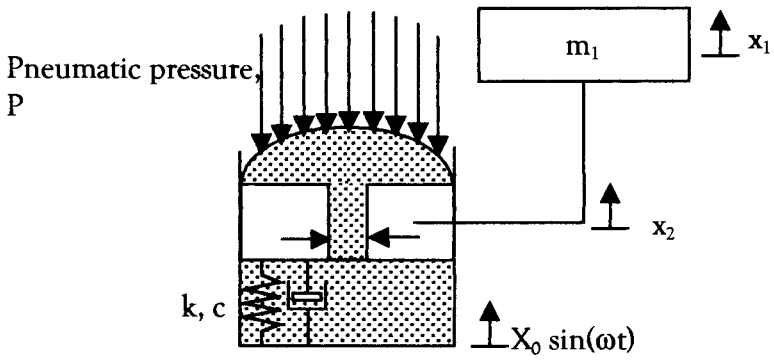

Figure 5.25: Schematic representation of absorber

To compensate for the fact that the MT frequency is below the isolation frequency on the frequency spectrum, the stiffness of the absorber has to be changed in order to move the MT frequency away from the drill operating frequency.

The stiffness change has been achieved by applying sufficient pneumatic air pressure above the diaphragm, as shown in Fig. 5.25. When applying the pressure, the system goes through a non-linear stage where the stiffness actually drops with an increase in air pressure. Thereafter, the stiffness of the system rises dramatically with further increase in air pressure. The transmissibility of the system measured at an air pressure of about 40 kPa is shown in Fig. 5.26.

As the figure shows, the stiffness has been increased from about 340 kN/m to 1.18 GN/m with an increase of 40 kPa in air pressure upon the diaphragm. This caused a 40 Hz jump in MT frequency. The figure also shows that the transmissibility will be much lower in the 0 to 28 Hz region with the air pressure applied. This will enable much more control of the drill during startup or hole collaring.

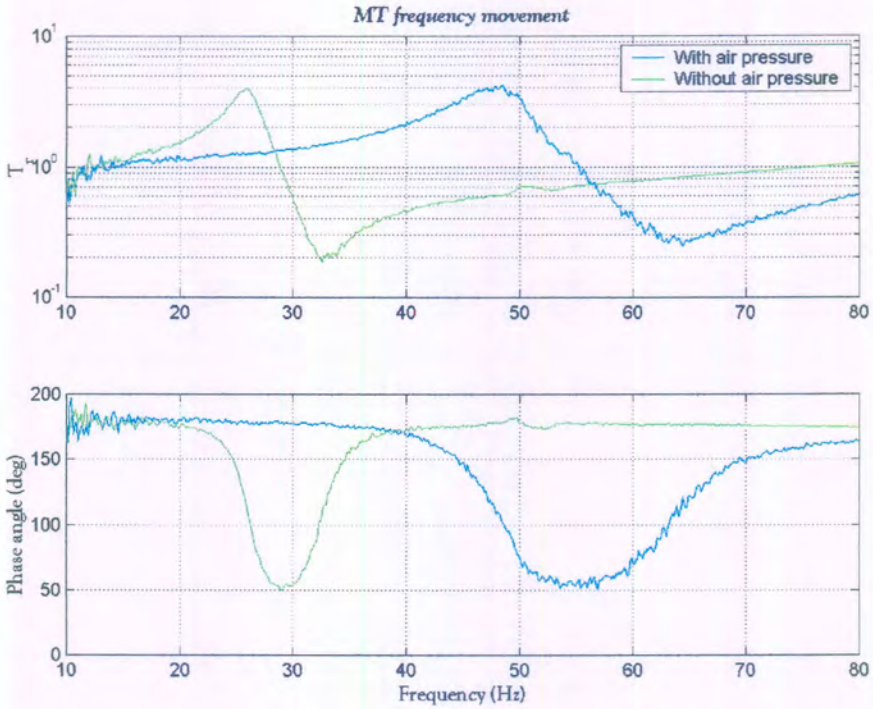

Figure 5.26: MT frequency movement due to air pressure increase

Compensating for minor changes in drill operating frequency.

The compensation for minor changes in the operating frequency was made by varying the air pressure behind the rubber diaphragm. The pressure differences were much smaller, and as a result, the control of the system was done in the highly non-linear region of the system. The reason for the non-linearity is mainly geometrical and is explained in Fig. 5.27.

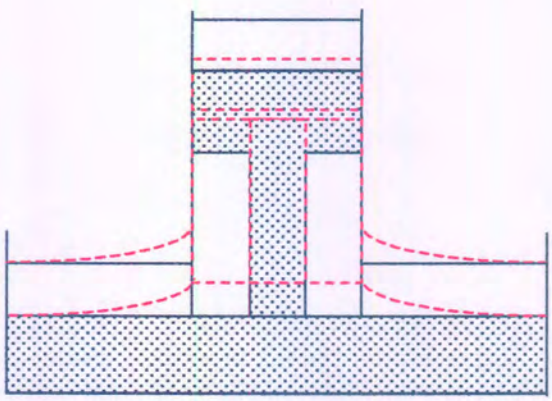

Figure 5.27: Geometrical non-linearity

The diaphragm has been modeled as a piston-cylinder configuration. The dotted lines represent the movement of the absorber port relative to the base. The handle is attached to the port, and will thus move with the port. When air pressure is applied upon the diaphragm, the port will move away from the base of the absorber. This forces the rubber into a non-linear position where the stiffness of the rubber is related to the position of the port.

This phenomenon makes the control system very difficult to analyse analytically. The governing equation for the pneumatic force due to air pressure is:

$$F_c(x) = \frac{P_o V_o^{\frac{1}{3}}}{(V_o - A_d x_d)^{\frac{1}{3}}} \qquad (5.6)$$

The variables P_o, V_o, A_d and x_d are the initial pressure, the initial volume above the diaphragm, the diaphragm area, and the movement of the diaphragm respectively. The equation shows that the system is non-linear in that the pneumatic force is a function of the movement of the diaphragm. It would not be a valid assumption to keep the value of x_d constant as a function of time or frequency. The diaphragm area, A_d, will also be a function of the diaphragm movement, because of the fact that the diaphragm moves down the throat of the port at the end of the downward stroke. The two variables, V_0, and P_0 have been varied by changing the volume above the diaphragm with a bellow type controller.

The pressure has been measured with a manometer, and measurements have been taken at 100 Pa intervals from 0 to 680 Pa. The isolation frequency has been moved down with about 8 Hz, and back up to ensure repeatability. Fig. 5.28 shows the control measurements. The excitation signal in this instance was a random signal with a peak to peak value of 1 mm and a frequency range between 10 and 90 Hz. The measurement quality is a bit lower than that plotted in Fig. 5.23, because of the non-linearity effects of increasing the air pressure behind the diaphragm.

Fig. 5.29 shows a plot of isolation frequency vs. air pressure. The isolation frequency actually drops with increasing pressure, which is somewhat different from what is expected, and from what eq. 5.6 suggests. The reason for this decrease in stiffness with increasing pressure cannot be explained mathematically at this stage and can only assumed to be related to the non-linear effects described in the previous paragraphs and the dynamics of the polyurethane as described in Fig. 5.27.

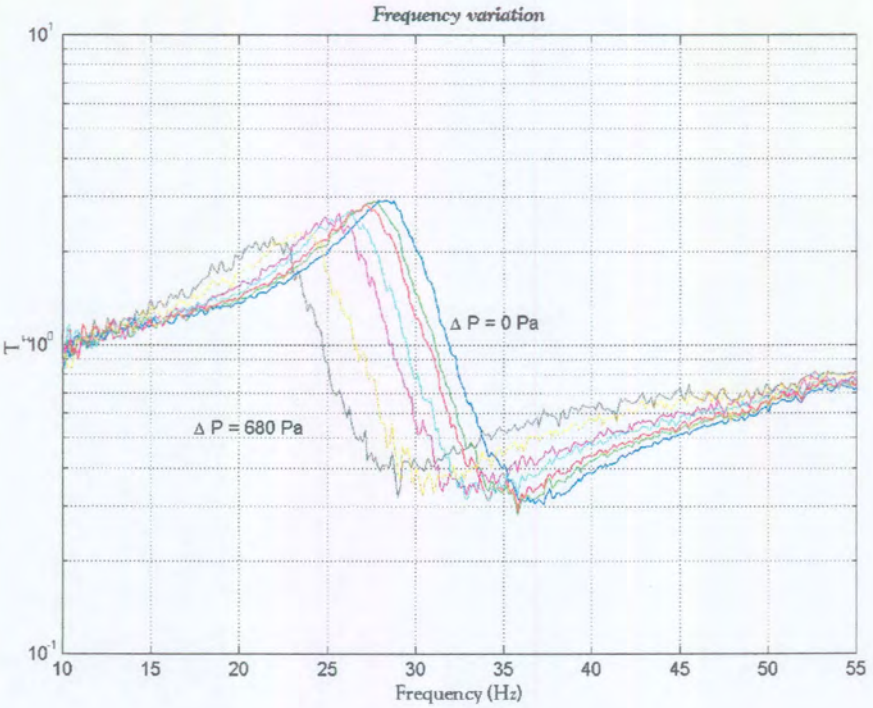

Figure 5.28: Control measurements

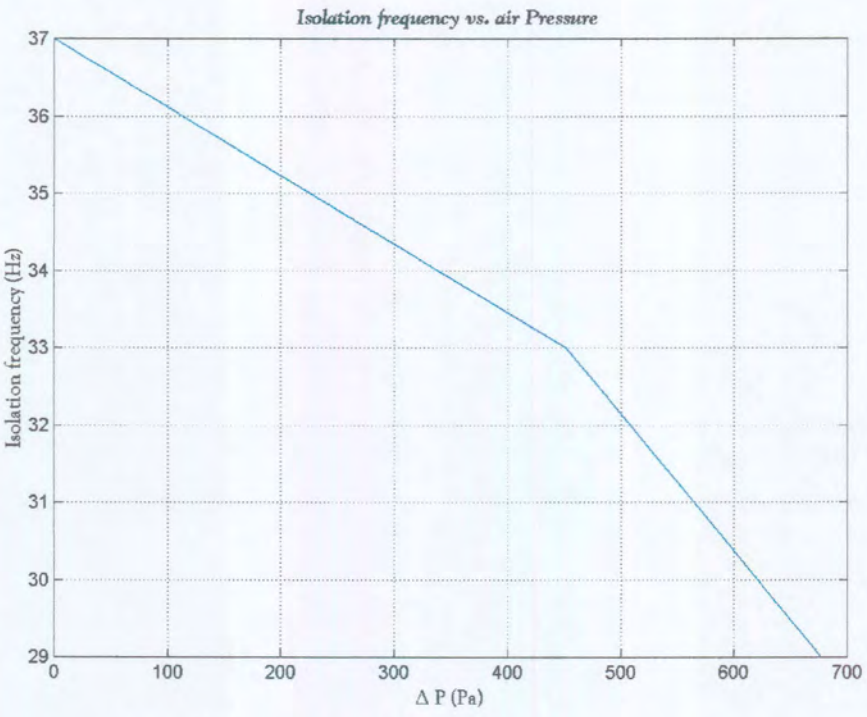

Figure 5.29: Isolation frequency change vs. air pressure

The stiffness thus reduces for pressure increases between 0 and 680 Pa. After 680 Pa the geometry of the polyurethane changes as described in Fig. 5.27, and the system becomes very stiff. Nevertheless, the result was evaluated with different diaphragms

and successfully tested for repeatability. Fig 5.30 shows a diagram of the control system. An important aspect to notice about Fig. 5.28 is that although the isolation frequency has only been moved by about 8 Hz, the frequency band between 26 and 44 Hz has a transmissibility lower than 60 %.

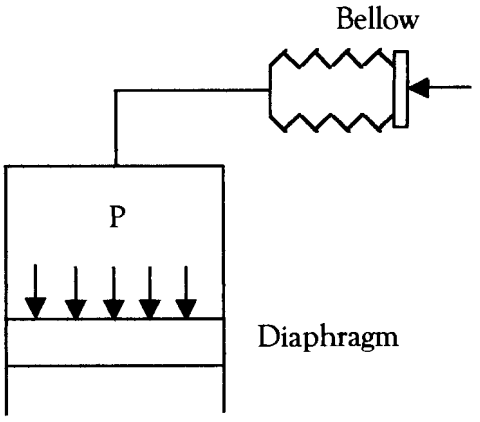

Figure 5.30: Diagram of control system

5.7 Comparison between experimental and theoretical results

Stiffness:
The stiffness of the polyurethane rubber has been analytically calculated in section 4.1 by using elementary plate theory. The calculated stiffness for the design as discussed in section 4 is 128 kN/m. This result can be verified by looking at the measurements where the absorber was tested without a working fluid. Fig. 5.10 shows the stiffness constant as a function of frequency for the system without fluid. At 10 Hz, the stiffness was calculated to be 115 kN/m. A static test was not done because of the fact that the rubber stiffness changes by a considerable amount as a function of frequency.

The theoretical estimation was thus quite adequate for a design that nearly has the same critical frequencies in theory and in practice.

The stiffness contribution of the diaphragm was considered to be much less than the stiffness of the polyurethane rubber. This, however, has proved not to be a very good assumption, even with latex rubber acting as a diaphragm. A reduction in port diameter has been used to compensate for this assumption, but this caused the transmissibility to increase slightly due to frequency ratio reduction and increased fluid damping. This effect can be witnessed in Fig. 5.22.

Damping:

Although damping is relatively difficult to quantify, an attempt has been made in section 4.2 to estimate the damping coefficient. The damping coefficient for the 20 mm port has been calculated to be 200 Ns/m for an amplitude of 0.5 mm and 245 Ns/m for an amplitude of 0.75 mm.

The damping coefficient measured for this configuration has been 366 Ns/m for an amplitude of 0.5 mm and 457 Ns/m for an amplitude of 0.75mm (See Fig. 5.17). The theoretical calculations must be corrected for the incorrect stiffness value of 128 kN/m that has been used for the structural damping coefficient calculation. The theoretical estimation for the damping coefficient after a corrected stiffness constant of 500 kN/m (see Fig. 5.17) has been used for the system, which has a MT frequency of 45 Hz, the theoretical estimation for the damping coefficient is 397 Ns/m.

Transmissibility

Various configurations have been tested, and the most critical parameters have been varied in the experimental procedure. It is important to verify that the measured transmissibility can be correlated with the theoretical prediction. It is also important to verify that the changes in parameters produced the same trends as had been predicted in the theoretical derivation.

The first verification is that of a theoretical transmissibility plot with a measured plot that has basically the same critical parameter values. Fig. 5.31 shows a comparison between theoretical results and experimental measurements for the large port, stiff configuration (see Fig. 5.13).

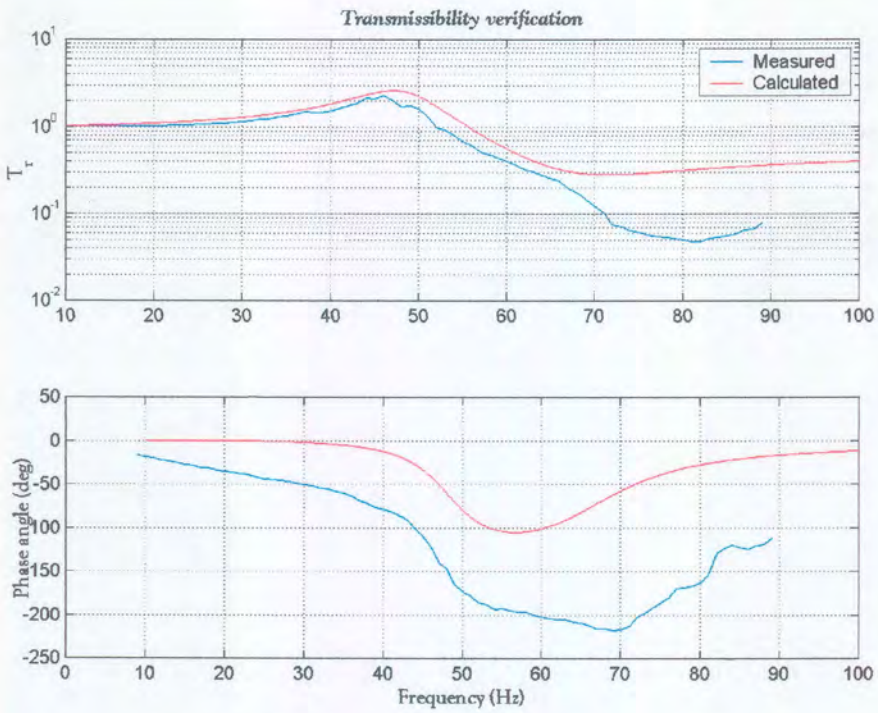

Figure 5.31: Theoretical vs. measured transmissibility

The theoretical calculation has been done with a revised stiffness constant of 650 kN/m extrapolated between the MT and isolation frequencies (See Fig. 5.18). The natural frequency of the theoretical result is thus a bit higher than the measured value. The isolation frequency of the theoretical result is lower than the isolation frequency of

the measured result because of a stiffness constant that increases with increasing frequency (Fig. 5.14).

The system response to a smaller port has also been verified theoretically and is shown in Fig. 5.32 together with the experimental analogue. The stiffness constant has been taken from Fig. 5.17 at 45 Hz as 1.2 GN/m.

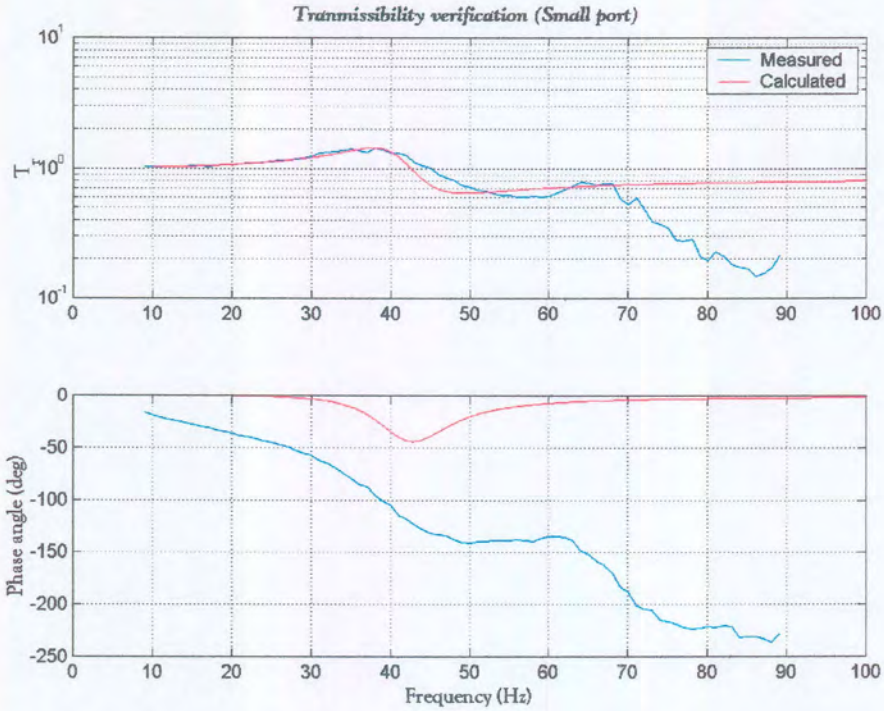

Figure 5.32: Small port verification

The transmissibility corresponds relatively well, except for the isolation frequency that deviates by 7 Hz because of a non-linear stiffness constant (Fig. 5.17). The phase angle differs quite noticeably, which is probably due to the phase difference between the two amplifiers mentioned previously in this chapter (see 5.5 Results: Acceleration measurements: P 83).

The system's response to density variation has also been investigated. The system has been tested and theoretically simulated with both water and methylated spirits. The density of methylated spirits has been measured as 840 kg/m^3. Fig. 5.33 and 5.34 show a comparative plot of the theoretical results vs. the measured responses. The stiffness constant for the system with the diaphragm used in instance, latex, has been measured and calculated as shown in section 5.5 as 260 kN/m.

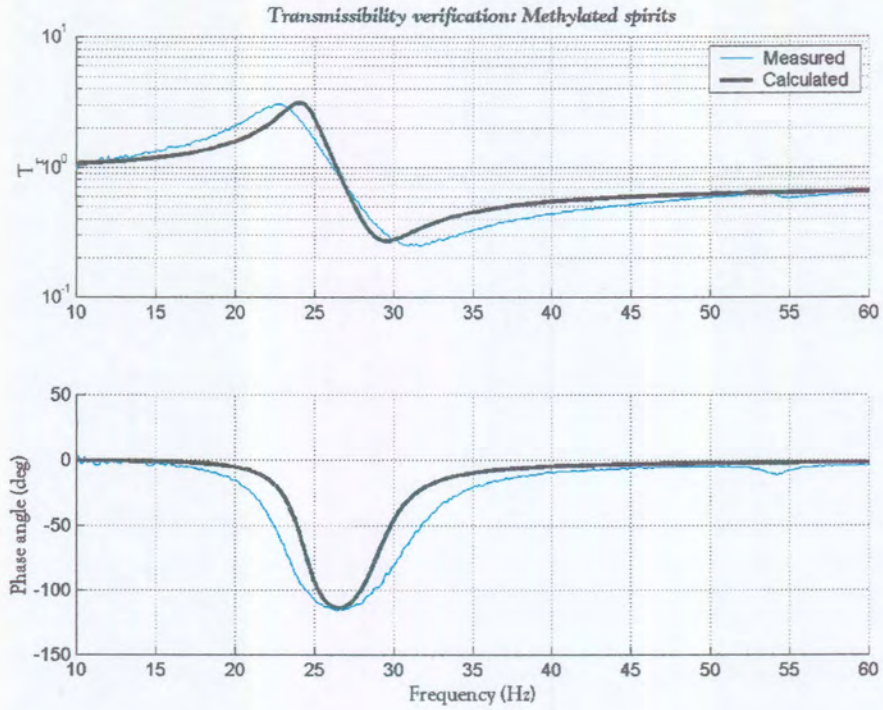

Figure 5.33: Transmissibility of system with spirits

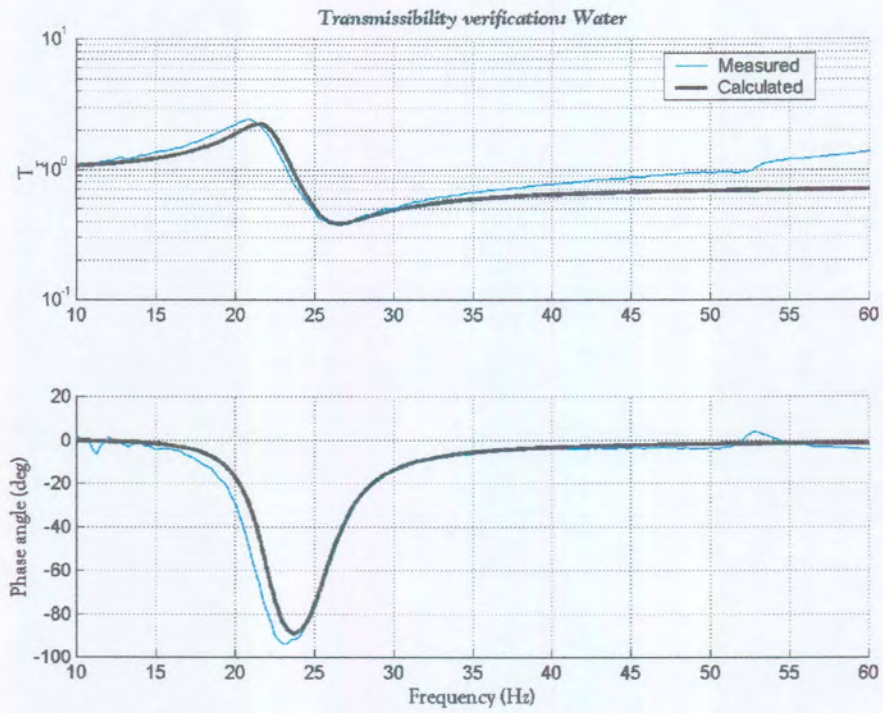

Figure 5.34: Transmissibility of system with water

The theoretical results is, as discussed in this section, are very accurate when the stiffness constant of the system is known. Damping constant will have to be determined experimentally, because a theoretical estimation is not satisfactory. The stiffness constant of the polyurethane rubber can, with the current geometery, accurately predicted by analytical formulas.

6. Conclusion

6.1 Accomplishments

The results have identified a definite isolation frequency, and the experimental verification has verified the analytical design and optimisation procedure. The analytical procedures can now be used with confidence to design this type of absorber in the future. The stiffness coefficient of the system must be known or accurately predicted.

The results have shown that the transmissibility can be reduced to between 20-40 % of the unattenuated rock drill handle transmissibility. The analytical procedures that have been presented can be used to design an absorber for a specific type of drill with a specific operating frequency. It has been proven that the stiffness of the system can be relatively high, even with a tool operating frequency below 50 Hz. This means that the operator will still have adequate control of the drill, whilst subjected to less vibration.

The MT frequency might be a problem during collaring and startup. As the MT frequency placement is somewhat troublesome, and difficult to position above the isolation frequency, it has been proposed that the concept must be able to compensate for this problem by moving the MT frequency higher up the frequency spectrum during collaring and startup. The results have shown that the MT frequency can be shifted with about 30-40 Hz upwards on the frequency spectrum by increasing the air pressure behind the diaphragm with about 40 kPa. This resulted in a very near unity transmissibility in the zero to operating frequency region. The absorber may thus be 'switched off' during the collaring or startup procedure.

In the problem statement it has been noted that the concept must be able to compensate for minor changes in the operating frequency of the drill. This is due to variations in pneumatic pressure, rock hardness etc. The experimental procedure has proven that it is possible to shift the isolation frequency with about 7 Hz by applying minor pressure changes to the diaphragm. The results have verified that this procedure is repeatable regardless of the port configuration or diaphragm type. Although the change is already a ±10 % shift in isolation frequency to both sides, the absorber functions over a relatively broad frequency band of attenuation. If Fig. 5.28 is studied, it will be noted that the absorber is able to reduce the transmissibility by more than 50% from 26 Hz to 45 Hz.

A serious disadvantage of the suggested control system however, is the fact that it could not be verified analytically due to the non-linear variables that play a role in the dynamics of the system. This makes the control system a bit unpredictable in the sense that the frequency band cannot be predicted in the design phase.

The major contributions of this thesis is the fact that the concept has been designed, manufactured, tested and proven for a given configuration. Adjustment of the isolation frequency is made possible by means of a pneumatic control system. The practical implications and problems of this type of attenuation has been defined and solved.

6.2 Aspects that require more research

A number of issues have been identified that warrants further research. An aspect that definitely requires more research is the characteristics of the polyurethane rubber. Aspects like the stiffness and damping dependency on frequency have to receive enough attention in order to make the design process more accurate and reliable. The analytical result for the static stiffness constant of the rubber is acceptable, but not sufficient. A stiffness – frequency dependency must be defined in order to predict the isolation frequency in the design phase.

More experimental work is required to confirm the structural damping constant of polyurethane to ensure that it is indeed the optimum material for the application. The structural damping constants for other elastomers must also be evaluated and compared, for this kind of information is limited in the literature today.

Another aspect that should receive more research is the optimum design of the diaphragm. The diaphragms used in this thesis have a flat, plate like geometry. It will be better to use a concave or even a bellow type geometry for the diaphragm. The reason for this is to ensure that the diaphragm only bends with the flow. With the current geometry the diaphragm actually has to 'blow up' and deform. This causes the stiffness of the system to be affected noticeably.

Although adequate isolation frequency shift has been achieved, more research should be concentrated on the control issue. The control system should be designed in such a way that the transmissibility, and the isolation and MT frequency ratio, is not affected noticeably. This fact makes a stiffness change very attractive, although a considerable change in stiffness is necessary to make an impact on the isolation frequency.

The stiffness of the designed absorber in the directions other than the drill operating frequency is not enough. The type and geometry of the structural rubber should be experimented with in an attempt to stiffen the absorber in these directions. A two- or three-dimensional absorber would also be a solution to this problem.